MAGNETIC CIRCULAR DICHROISM STUDIES OF HEMOGLOBIN

THE REDUCTION OF FERRIHEMOGLOBIN BY FERROCYTOCHROME b_5 AND CHARACTERIZATION OF THE HIGH-SPIN HYDROXY SPECIES OF MIXED-VALENCE HEMOGLOBIN

David A. JUCKETT * and Donald E. HULTQUIST

Department of Biological Chemistry, University of Michigan School of Medicine, Ann Arbor, MI, U.S.A.

The final step in the erythrocyte methemoglobin reduction pathway, the transfer of an electron from cytochrome b_5 to methemoglobin, has been studied using magnetic circular dichroism spectroscopy. Spectral analysis allowed us to determine accurately the concentration of each redox species in mixtures of the two heme-proteins and to follow simultaneously the kinetics of the appearance or disappearance of each of these species during reduction reactions. Our analysis detected a substantial increase in the high-spin hydroxymethemoglobin species in the partially reduced bovine hemoglobin tetramer. This species was sensitive to the degree of reduction and pH, and was spectrally similar to fluoride methemoglobin. At pH 7.8, 100% of the hydroxide component of methemoglobin was in the high-spin form when two or more subunits were in the ferrous form. Kinetic analysis of bovine methemoglobin reduction yielded values for the apparent first-order rates for the tetrameric species possessing four, three, two, and one ferric subunit. Further analysis showed that the reduction kinetics can also be described by an equilibrium state, pure competitive inhibition model for enzyme catalysis in which ferrous and ferric subunits of hemoglobin compete for cytochrome b_5. This analysis generated a K_D that depends on ionic strength and hemoglobin tetramer conformation, a V_{max} that was independent of these factors, and an inhibition constant that was equal to K_D. This model is consistent with the hypothesis that the reduction of methemoglobin can be separated into two steps, the ionic interaction between cytochrome b_5 and hemoglobin and the electron transfer.

1. Introduction

Magnetic circular dichroism (MCD) spectroscopy has been used to study a number of heme-proteins, including cytochrome b_5 and hemoglobin [1–7]. The MCD spectra of these heme-proteins have been shown to be very sensitive to spin, oxidation, and ligand states of the heme. The visible region of the reduced cytochrome b_5 spectrum contains a very sharp, intense A term [2] which allows small concentrations of this species to be detected in the presence of other heme-proteins [3]. Hemoglobin MCD spectra show unique differences with various ligands in both the oxidized and reduced states [4–7].

Evidence that cytochrome b_5 and methemoglobin form a complex has been provided by isoelectric focusing studies [8], by kinetic studies of the transfer of electrons from ferrocytochrome b_5 to methemoglobin [9], and by spectral perturbation in the visible region of the ferric forms of hemoglobin and solubilized liver microsomal cyto-

---

* Present address: Department of Biochemistry, St Jude Children's Research Hospital, 332 N. Lauderdale, P.O. Box 318, Memphis, TN 38101, U.S.A.

chrome b_5 [10]. The significance of such a complex lies with the observation that methemoglobin reduction by the enzymatic system of erythrocytes proceeds through such a complex and that the rate of methemoglobin reduction under physiological conditions appears to be dependent on the concentration of the complex [9].

In this study we have further examined the interaction of reduced cytochrome b_5 with hemoglobin and described the results in terms of two models. A nonreversible first-order model fits the data and yields values of the rate constants for tetrameric hemoglobin species possessing four, three, two and one ferric subunit. A Michaelis-Menten equilibrium state model describes the data well in terms of formation of a cytochrome b_5-ferric hemoglobin complex, electron transfer between hemes of this complex, and competition between ferrous and ferric hemoglobin subunits for the cytochrome. During the reduction to deoxyhemoglobin, we observed in mixed-valence hemoglobin the conversion of hydroxymethemoglobin subunits to a pure high-spin species with an MCD spectrum similar to that of fluoromethemoglobin.

2. Materials and methods

2.1. Materials

NAD, NADH, Bis-Tris, and Trizma base were obtained from Sigma Chemical Co. Horse heart myoglobin was obtained from ICN Biochemicals. Bovine liver microsomal cytochrome b_5 reductase was obtained by the method outlined previously [11] and was solubilized with chymotrypsin by the method of Spatz and Strittmatter [12]. Bovine liver microsomal cytochrome b_5 was purified by the method of Ozols [13]. The cytochrome b_5 was incubated with bovine liver lysosomal cathepsin D and the resulting solubilized cytochrome was purified to near-homogeneity by chromatographic procedures (Schafer, Peters and Hultquist, unpublished data). Bovine hemoglobin was isolated from fresh blood (purebred Hereford) by the method of Antonini and Brunori [14] and was further purified on DE-52 cellulose. The hemoglobin was bound to the column at pH 8.6 in a Tris-Cl buffer

of ionic strength 0.02 M. Bovine hemoglobin A was then eluted with a decreasing pH buffer at constant ionic strength.

Hemoglobin was oxidized with a 3–4-fold excess of potassium ferricyanide in a buffered solution. The solution was then passed through Amberlite MB-3 (Sigma) mixed-bed ion-exchange resin to remove all ions. Methemoglobin was stored at 4°C at a concentration of about 2 mM and was used within 5 days. All methemoglobin and hemoglobin concentrations are expressed on a per heme basis.

2.2. Apparatus and data collection

MCD spectra were taken on a Jasco J-40C spectropolarimeter equipped with an electromagnet capable of generating a field strength of 15 000 G. The spectropolarimeter was interfaced to a Nova III computer and a Tracor 1500N signal analyzer. Spectra acquisition, storage and baseline subtraction were facilitated by the computer/ signal analyzer pair. The spectra consisted of 1024 data points which were fed out to an Ohio Scientific Challenger II microcomputer which then stored the spectra on floppy disks. Each scan was condensed to 128 points, for subsequent multiple linear regression analysis, by averaging eight adjacent points sequentially along the spectrum. All spectral analysis and plotting was performed on the Challenger II using basic programs and an ADM 3a terminal retrofitted with the Retro-Graphics plotting hardware.

Spectra were obtained from the spectropolarimeter at 50 nm/min, with the sensitivity scale set at 20 mdegree/cm, a 1.0 time constant, 1 nm spectral bandwidth, 15 000 G magnetic field, and the sample temperature of 4–8°C. Baselines were scanned four to six times, averaged, and then stored in the Nova/Tracor. Anaerobic cuvettes with path lengths of 1 cm and 2 mm were used. A single spectrum containing MCD plus CD was obtained at each time point during an enzymatic reduction. The natural CD in the 670–470 nm range was very small for hemoglobin, myoglobin, and cytochrome b_5 and did not interfere with the analyses.

2.3. Methemoglobin reduction

Methemoglobin was reduced by the electron-transport chain consisting of NADH, protease-solubilized microsomal cytochrome b_5 reductase and protease-solubilized microsomal cytochrome b_5 in 20 mM Bis-Tris ($I = 3$ mM), pH 7.3, in the absence and presence of NaCl and inositol hexaphosphate (IHP). We used concentrations of components that maintained cytochrome b_5 primarily in a reduced form in the presence of methemoglobin. This allowed us to examine the transfer of electrons from cytochrome b_5 to hemoglobin with the proteins in the physiologically relevant redox states. Hemoglobin concentrations were maintained at 50 μM or greater to assure a minimum of 90% of the hemoglobin in the tetramer form at the highest ionic strength used. We used the value of 4×10^6 M^{-1} for the dimer-tetramer association constant of bovine hemoglobin [15] (derived for an ionic strength of 0.225 M) to arrive at this lower limit.

Under aerobic conditions, NADH was added to a mixture of the proteins to start the reaction. Under anaerobic conditions, hemoglobin was placed in the sidearm of a Thunberg cuvette and the remaining components placed in the main body of the cuvette. The cuvette was then repeatedly evacuated and flushed with N$_2$ which had been purified through an activated Ridox (Fisher Scientific) column and then bubbled through distilled water. Any residual O$_2$ was scrubbed from the system by the oxidation of ferrous cytochrome b_5. After approx. 1 h the methemoglobin was tipped in and its reduction was followed by MCD at 8°C. MCD spectra (duration of scan = 4 min) were taken at 5-min intervals after the initiation of the enzymatic reductions and were continued until most of the methemoglobin was reduced.

2.4. Data analysis

The relative contributions of the 'pure' oxidation states of the heme-proteins present in a sample spectrum were determined using multiple linear regression analysis. The spectra of the pure states were used as the independent variable ($X_i(j)$) in the equation:

$$Y(j) = a_0 + a_1 X_1(j) + a_2 X_2(j) + \ldots + a_n X_n(j) \tag{1}$$

where j represents the number of data points in each spectrum and therefore the number of data sets ($Y, X_1, X_2, \ldots X_n$) used in the regression analysis.

Due to a slight drifting in the monochrometer, the MCD signals were shifted as a function of time. It was necessary to analyze for this shift because the standard spectra (X_i) and sample spectra were taken at times which differed by hours or days. Since the shifts were small (< 2 nm) we obtained a first-order approximation of the shift of a standard spectrum by including its first derivative in eq. 1 as an additional independent variable. This led to the equation:

$$Y = a_0 + a_1 X_1 + a_2 X_2 + \ldots + b_1 \frac{dX_1}{d\lambda}$$

$$+ b_2 \frac{dX_2}{d\lambda} + \ldots \tag{2}$$

The coefficient b_i was divided by a_i to determine the shift, $\Delta\lambda_i$; the shift is determined from the coefficient of the first derivative of the contribution of X_i to the sample spectrum, which is $\Delta\lambda_i \mathrm{d}(a_i X_i)/\mathrm{d}\lambda$. Since this term is equivalent to $\Delta\lambda_i a_i \mathrm{d}X_i/\mathrm{d}\lambda$, $b_i = \Delta\lambda_i a_i$, and $\Delta\lambda_i = b_i/a_i$. Analysis for shifts was routinely included only on the standard spectra of reduced cytochrome b_5 and oxyhemoglobin because of the narrow, intense bands in these spectra.

It was occasionally necessary to reduce the number of independent variables in eq. 1. Since the oxidized and reduced forms of a single protein species are related to the total amount of that protein by the equation $c = a_1 + a_2$, the value of $c - a_1$ can be substituted for a_2 in eq. 1 or 2 where the subscripts 1 and 2 represent oxidized and reduced species of a single protein, respectively. This substitution yields an equation with one less independent variable and one less degree of freedom. The equation to be solved is then:

$$Y - cX_2 = a_0 + a_1(X_1 - X_2) + a_3 X_3 + \ldots \tag{3}$$

(This general form can be expanded for use when more than one pair needs to be set equal to a

constant.) The use of this equation can be advantageous when the spectrum of one of the protein species is of low intensity, or when it resembles the spectral characteristics of a species from another protein. If a low-intensity species has a complementary redox state with a highly intense, highly unique signal, then use of eq. 3 couples the evaluation of the coefficients a_1 and a_2 to the highly unique species and thereby gives a more accurate determination of the less unique signal. Even with hemoglobin present in a 10-fold excess, the weak signal of oxidized cytochrome b_5 was successfully determined by coupling it to the highly intense reduced cytochrome b_5 signal.

The computer algorithm for the multiple regression analysis was adapted from that of Bevington [16]. Incorporation of the first derivatives and the coupled solutions originated with the authors.

2.5. Kinetic analysis model I: A sequential, first-order approach

A simple, first-order model was used to predict the reduction of each subunit of the methemoglobin tetramer. This model was based on the scheme:

$$H_4 \xrightarrow{k_4} H_3 \xrightarrow{k_3} H_2 \xrightarrow{k_2} H_1 \xrightarrow{k_1} H_0$$
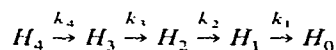
where the H_i represent the concentrations of tetramer with i subunits in the ferric state. Since each step is first-order it follows, therefore, that

$$dH_i(t)/dt = -k_i H_i(t) \tag{4}$$

At time zero, all the hemoglobin is in the ferric form (i.e., H_3, H_2, H_1 and H_0 equal zero). The amount of total ferric heme as a function of time is represented by

$$Fe^{3+}(t) = \sum_i iH_i(t), \quad i = 4,3,2,1 \tag{5}$$

The concentration of each tetrameric species can be numerically estimated by the following set of equations:

$$H_4(t + \Delta t) = H_4(t) + \Delta H_4(t) \tag{6a}$$

$$H_i(t + \Delta t) = H_i(t) + \Delta H_i(t) - \Delta H_{i+1}(t)$$
$$i = 3,2,1 \tag{6b}$$

and

$$H_0(t + \Delta t) = H_0(t) - \Delta H_1(t) \tag{6c}$$

where

$$\Delta H_i(t) = -k_i H_i(t)\Delta t, \tag{6d}$$

Eqs. 5 and 6 were used to generate the smooth curves in fig. 3 after estimates of k_i were obtained.

This reaction scheme can also be integrated into an exact analytical form [17] that directly gives each H_i as a function of time. The integrated rate equations were used in an iterative least-squares method described by Olson [17] to arrive at estimates of k_i using the experimentally measured data, $Fe^{3+}(t)$. The estimates of k_i were obtained by minimizing a computed error function containing $k_i + \Delta k_i$ and then solving for Δk_i. This procedure was performed iteratively until the k_i terms converged to stable values. This method required initial guesses of k_i and they were often the critical factor determining convergence. It was also apparent that local minima existed in the 'solution space' for the four k_i terms that resulted in convergence to slightly different values depending on the initial guesses. We, therefore, cannot be sure that the estimates of k_i given here represent the true global minimum for each data set but they are adequate estimates because in all cases the differences between the four k_i terms of a solution were very much greater than the slightly different values obtained for each k_i with various initial guesses.

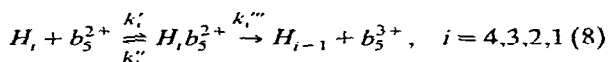### 2.6. Kinetic analysis model II: An equilibrium kinetics, competitive inhibition approach

An equilibrium state, pure competitive inhibition formulation was also used to describe the kinetic data for reduction of methemoglobin. This model assumes that cytochrome b_5 takes the role of enzyme, methemoglobin is the substrate, and ferrous hemoglobin is a pure competitive inhibitor. The velocity equation for an increase in the total ferrous heme, Q, can be constructed as the sum of velocity components for each valence form of the tetramer and is given by:

$$\frac{dQ}{dt} = \frac{V_{max}}{4} \left\{ \frac{4H_4}{K_D + \frac{K_D}{K_I}Q + H_4} + \frac{3H_3}{K_D + \frac{K_D}{K_I}Q + H_3} \right.$$

$$+ \frac{2H_2}{K_D + \frac{K_D}{K_I}Q + H_2} + \frac{H_1}{K_D + \frac{K_D}{K_I}Q + H_1} \Bigg\}$$

$$(7)$$

where V_{max} is the maximum velocity for reaction of cytochrome b_5 with a fully oxidized hemoglobin tetramer, H_i the concentrations of hemoglobin tetramer with i oxidized subunits, K_I the inhibition constant arising from the nonproductive complexation of ferrous cytochrome b_5 with a ferrous hemoglobin subunit, and K_D the dissociation constant characterizing the complexation of ferrous cytochrome b_5 with a methemoglobin subunit. The degree of inhibition by ferrous subunits increases with increasing [Q] which is a common factor in all terms while substrate concentration H_i for each term depends on the instantaneous amount of that tetrameric form. The factors 4, 3, 2 and 1 are incorporated because of the reactivity cross-section of the various tetramer forms, thus, eq. 7 contains three unknown parameters, V_{max}, K_D and K_I, each with an intrinsic meaning within the framework of the model.

This model was derived using Michaelis-Menten kinetics under equilibrium conditions as applied to the following reaction scheme:

$$H_i + b_5^{2+} \underset{k_i''}{\overset{k_i'}{\rightleftharpoons}} H_i b_5^{2+} \overset{k_i'''}{\rightarrow} H_{i-1} + b_5^{3+}, \quad i = 4,3,2,1 \quad (8)$$

where b_5^{2+} and b_5^{3+} represent the ferrous and ferric forms of the cytochrome. (Under the conditions of this work, the concentration of b_5^{3+} is negligible.) Eq. 7 was derived from this reaction scheme under the assumption that each rate constant in eq. 8 is the same for all values of i and that equilibrium conditions are appropriate. The latter assumption requires that $k'' \gg k'''$ and therefore yields a K_D instead of a K_M as in the typical steady-state kinetic expression. (Using the V_{max} and K_D values derived in this work and a very conservative lower limit estimate of $k' = 1 \times 10^6$ M^{-1} s^{-1}, k'' is greater than k''' by at least 2 orders of magnitude for all the conditions studied.) The validity of these two assumptions was examined by trying to fit eq. 7 to the data using $\Delta Q/\Delta t$ and values of H_i generated by eqs. 5 and 6 obtained with the best-fit

values of k_i. Since the kinetic curves generated by using k_i (section 2.5) excellently reproduced the actual data, they served as an ideal way to obtain approximations to H_i and to obtain more accurately $\Delta Q/\Delta t$ by making Δt smaller than the time interval between actual data points. The value of V_{max} was obtained from the Lineweaver-Burk plot (fig. 4) and K_I was set equal to K_D, representing the most simple case for the interaction of the two proteins *. With V_{max} fixed and H_i and $\Delta Q/\Delta t$ generated for each time point, the test of eq. 7 simplified to the ability of a single K_D value to satisfy the equation at all points in the reduction. A K_D value can be generated for each time point by solving eq. 7 for K_D. This was done by rewriting eq. 7 as a fourth-order polynomial in K_D and determining the four roots at each time point. In all cases examined, only one of the four roots was positive and that was taken as the physically relevant solution. The roots obtained are shown in fig. 5 and described in section 3.2.

2.7. Elucidation of high-spin hydroxymethemoglobin

Spectra taken during the course of reductions were initially analyzed assuming that hemoglobin was present only as deoxyhemoglobin and methemoglobin, as represented by the spectra of pure deoxyhemoglobin and pure methemoglobin at the pH of the reduction. This type of analysis yielded values for the contributions of these two hemoglobin species at each point in the reduction. The sum of methemoglobin and deoxyhemoglobin at each point did not equal the total hemoglobin present, however, and the residual spectrum (the sample spectrum, Y, minus the computed contributions of known components) was not flat. These observations indicated that at least one other unique species was present in the MCD spectrum during reduction. The maximum deviation from a

---

* The inhibition constant, K_I, incorporated in eq. 7 represents a dissociation constant for the nonproductive complexation of ferrous cytochrome b_5 with a ferrous hemoglobin subunit. Since eq. 7 was derived using equilibrium rather than steady-state kinetics, it contains K_D which is the dissociation constant for the productive complexation of the two proteins. Both K_I and K_D are equilibrium constants and therefore it is reasonable to test the case where $K_I = K_D$.

best fit resulting from the unknown species oc-
curred midway through the reduction under
anaerobic conditions.

The spectrum of the unknown species was de-
termined by manipulation of the contributions of
met and deoxy forms of hemoglobin in such a way
that the following equations were satisfied at each
time point in the reduction:

$$a_1 \epsilon_{met}(\lambda) + a_2 \epsilon_{deoxy}(\lambda) + a_3 \epsilon_{unk}(\lambda) = A_{obs}(\lambda) \quad (9)$$

$$a_1 + a_2 + a_3 = [Hb]_{total} \quad (10)$$

where the $\epsilon(\lambda)$ terms represent the MCD spectra
(in units of $[\theta]_M$) for each species and A_{obs} is the
observed MCD spectrum at each time point. Since
a_1, a_2, a_3 and $\epsilon_{unk}(\lambda)$ were not known, an iterative
approach was used by varying a_1 and a_2 and using
the residual spectrum from the previous iteration
as $\epsilon_{unk}(\lambda)$. This proceeded until the $\epsilon_{unk}(\lambda)$ ob-
tained plus $\epsilon_{met}(\lambda)$ and $\epsilon_{deoxy}(\lambda)$ could be used to
fit all the time points of the reduction while
simultaneously satisfying eq. 10.

Since the unknown spectrum resembled high-
spin fluoromethemoglobin, the latter spectrum was
routinely used in all spectral analyses reported
here.

3. Results

3.1. MCD spectra of hemoglobin and cytochrome b₅

The MCD spectra of various ligand and valence
states of bovine cytochrome b₅ and hemoglobin
are shown in fig. 1 for the wavelength regions
370–470 and 470–670 nm. The spectra illustrate
the sensitivity of MCD to ligand and spin state of
the heme-proteins. For all of the protein states
shown, the visible region has more characteristic
band features than the Soret region. The spectra in
the visible region were used, therefore, in the mul-
tiple regression analysis to determine relative
oxidation state contributions of hemoglobin and
cytochrome b₅ during reduction.

3.2. Methemoglobin reduction

Reduction of methemoglobin was carried out
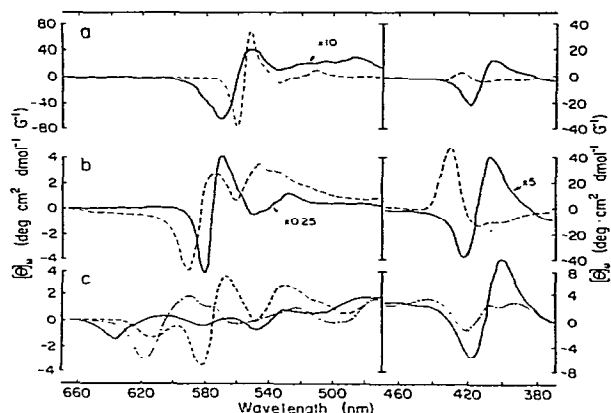under conditions which kept the cytochrome b₅ in

Fig. 1. MCD spectra of various forms of hemoglobin and
cytochrome b₅. Final concentrations: 10 μM cytochrome b₅
and 40 μM hemoglobin in 20 mM Bis-Tris (pH 7.3) at 8°C.
Ferrous species were obtained by addition of dithionite.
Methemoglobin was prepared as described in section 2.1. Top:
reduced cytochrome b₅ (— — —), oxidized cytochrome b₅
(———). Middle: oxyhemoglobin (———), deoxyhemoglobin
(— — —). Bottom: aquomethemoglobin (———), fluoro-
methemoglobin prepared in the presence of 100 mM NaF
(·—·—·), mixed-spin hydroxide methemoglobin at pH 10
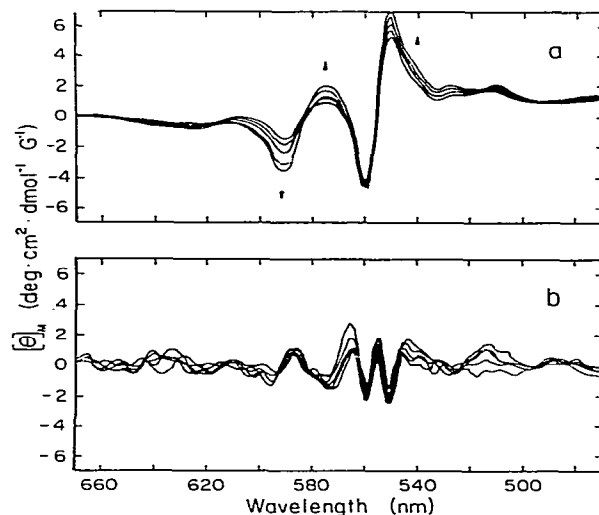(— — —).

Fig. 2. MCD spectral analysis of methemoglobin reduction. (a)
Spectra at selected times during reduction in the absence of
oxygen. Arrows indicate spectral changes with time. Specific
data are listed in table 1. (b) Residual spectra at the same time
points computed after best-fit analysis by linear regression.

Table 1

Results of the multiple regression analysis of reduction of methemoglobin and ferricytochrome b_5 under anaerobic conditions

Reaction conditions: 8°C, pH 7.4; final concentrations: 0.1 M NaCl, 7 mM Bis-Tris buffer, 1 mM NADH, and 0.05 unit cytochrome b_5 reductase/ml.

Time (min)	Concentrations (μM)						Shift (nm) of cytochrome b_5	$\dfrac{F^--Fe^{3+} Hb}{Total\ Fe^{3+}\ Hb} \times 100$ (%)
	H_2O-Fe^{3+} Hb	F^--Fe^{3+} Hb	Fe^{2+} Hb	O_2-Fe^{2+} Hb	Total Hb	$Fe^{2+} b_5$		
2	36.1	1.9	6.7	0.66	45.4	4.41	−0.17	5
7	27.4	4.8	13.2	0.42	45.8	4.68	−0.12	15
12	23.0	5.4	17.0	0.44	45.8	4.83	−0.15	19
17	20.6	5.8	19.4	0.47	46.3	4.87	−0.16	22
32	15.8	5.4	24.1	0.55	45.8	4.97	−0.02	25
52	13.8	4.2	28.0	0.57	46.6	5.01	−0.31	23
97	9.5	3.3	33.2	0.87	46.9	4.99	−0.19	26
147	6.7	1.6	36.2	1.20	45.7	4.96	−0.19	19

virtually a completely reduced state as demonstrated in fig. 2a. The intensity of the signal of the reduced cytochrome b_5 (near 555 nm) remained approximately constant as methemoglobin underwent complete reduction to deoxyhemoglobin. Maintenance of cytochrome b_5 in the ferrous form was crucial to the study of the final step in the electron transfer to methemoglobin and the kinetics described in this section were interpretable only if this condition was strictly met. The complete analysis of the reduction of fig. 2a is given in table 1. Using fluoromethemoglobin as an analog of the high-spin hydroxymethemoglobin species (see sections 2.7 and 3.3), a self-consistent analysis resulted, with total hemoglobin constant to within 1.1% standard deviation. The correction for the shift of the reduced cytochrome b_5 spectrum was small but necessary for a good fit. The residual
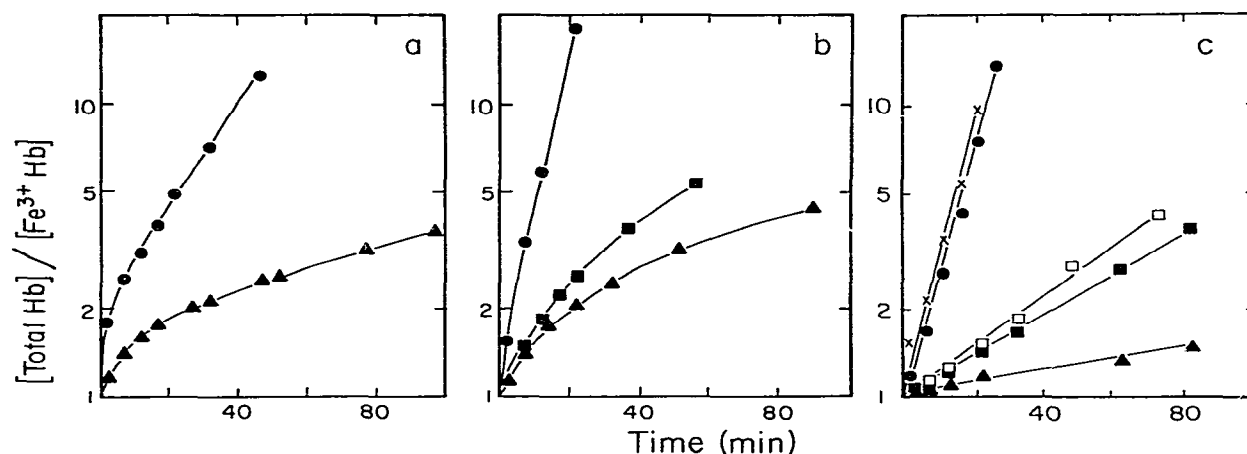

Fig. 3. Reduction of methemoglobin and metmyoglobin. The course of reaction is plotted such that slope is directly proportional to rate. Final concentrations: 0.01 unit of cytochrome b_5 reductase/ml, 1 mM NADH, and 20 mM Bis-Tris (pH 7.3). (a) Anaerobic reduction of methemoglobin. Final concentrations: 50 μM methemoglobin and 5 μM cytochrome b_5. No addition (●————●), 0.1 M NaCl (▲————▲). (b) Aerobic reduction of methemoglobin. Final concentrations: 50 μM methemoglobin and 5 μM cytochrome b_5. No addition (●————●), 0.04 M NaCl (■————■), 0.10 M NaCl (▲————▲). (c) Reduction of horse heart metmyoglobin. Final concentrations: 20 μM metmyoglobin and 1 μM cytochrome b_5. Anaerobic, no NaCl (×———×); anaerobic, 0.03 M NaCl (□————□); aerobic, no NaCl (●————●); aerobic, 0.03 M NaCl (■————■); aerobic, 0.1 M NaCl (▲————▲).

spectra resulting from this analysis were essentially flat, except for some deflections in the 560 nm region which were due to a slight narrowing (0.5–1.0 nm) of the ferrocytochrome b_5 signal during reduction (fig. 2b). The use of MCD and our analysis provided a suitable method to follow the various species involved in the reduction.

Time courses for the reduction of methemoglobin and metmyoglobin as a function of oxygen and ionic strength are shown in fig. 3. The data, plotted as ln([total subunits]/[ferric subunits]) vs. time, would yield straight lines for those reactions that follow first-order kinetics. The plots of methemoglobin reduction do not yield straight lines but rather lines with slopes that decrease as a function of time (fig. 3a and b). The slopes decrease with increasing ionic strength and there is a distinct biphasic nature to the anaerobic reduction. The plots for metmyoglobin, in contrast, appear to be first order with similar rates for aerobic and anaerobic conditions.

Analysis of the methemoglobin reduction kinetics using model I (as described in section 2.5) yielded four apparent first-order rate constants (designated k_4, k_3, k_2 and k_1) for the reduction of tetrameric hemoglobin possessing four, three, two, and one ferric subunit, respectively (table 2). These derived rate constants decreased in magnitude as the hemoglobin tetramer became more reduced. The smooth curves drawn through the data points in fig. 3a and b were generated from the derived rate constants k_i using eqs. 5 and 6a–d. The derived curves show an excellent fit to the experimental data. The average deviation of these curves from the data points is approx. 0.2%.
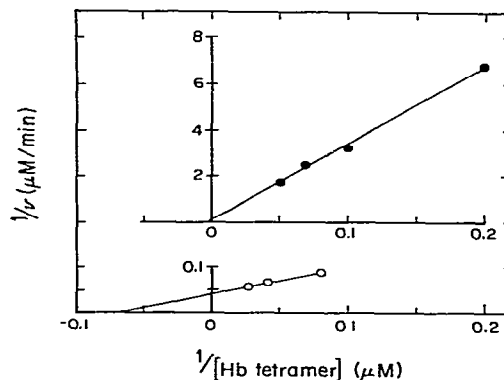

Fig. 4. Effect of methemoglobin concentration on the rates of electron transfer from ferrocytochrome b_5 to hemoglobin with 100 or 10% of the subunits in the ferric form. Reduction was carried out in the absence of oxygen with final concentrations of 1.0 mM NADH, 20 mM Bis-Tris buffer (pH 7.3), 0.05 unit cytochrome b_5 reductase/ml, 5 μM cytochrome b_5, and total hemoglobin concentrations varying from 12.5 to 50 μM hemoglobin tetramer. Lineweaver-Burk plots are shown for the initial velocities (O——O) and for the velocities at 90% reduction (●——●). At 90% completion, the calculation of concentration of tetramer containing one ferric subunit was based on the assumption that no more than one ferric subunit was present per tetramer.

The kinetics of reduction (fig. 3) were also analyzed using model II (as described in section 2.6) and values were obtained for K_D, K_1 and V_{max} which satisfied eq. 7 and reproduced the data. Values for V_{max} were obtained from the Lineweaver-Burk plots (fig. 4) which represent velocities taken from the initial and final regions of reductions carried out with different total hemo-
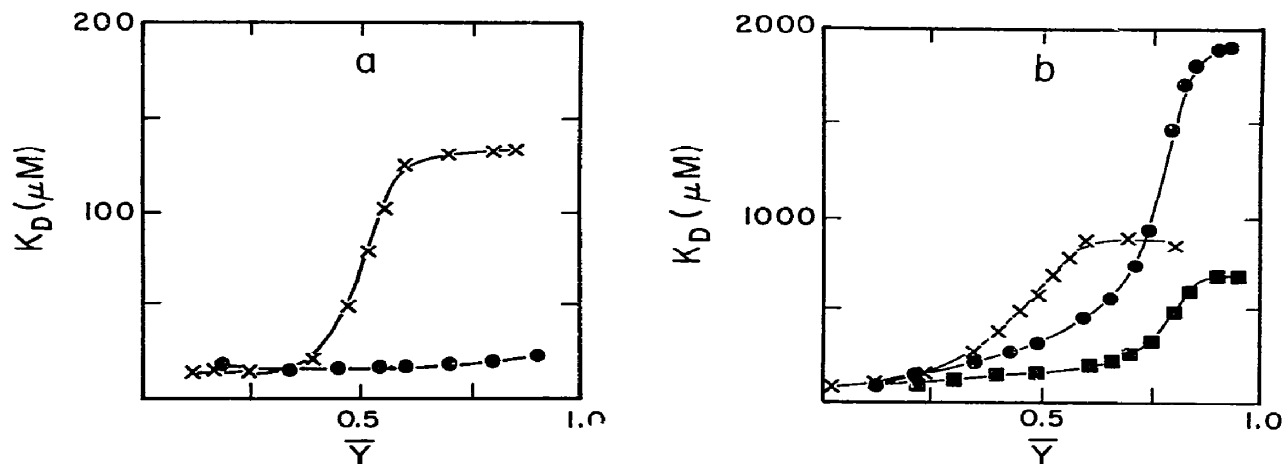
Table 2

Apparent first-order rate constants for reduction of each valence species of tetrameric methemoglobin

For conditions and concentrations see fig. 3.

O_2	Ionic strength (M)	Apparent rate constants (min^{-1})			
		k_4	k_3	k_2	k_1
+	0.003	0.985	0.600	0.285	0.099
+	0.043	0.317	0.110	0.085	0.010
+	0.103	0.269	0.090	0.034	0.004
−	0.003	1.25	0.800	0.092	0.039
−	0.103	0.312	0.080	0.013	0.011

Fig. 5. Effect of degree of reduction, $\bar{Y}$, on K_D. K_D were determined as described in section 2.6. (a) Low ionic strength (0.003 M). Aerobic conditions (●————●), anaerobic conditions (×————×). (b) Higher ionic strength. $\mu = 0.1$ M, aerobic conditions (●————●); $\mu = 0.1$ M, anaerobic conditions (×————×); $\mu = 0.043$ M, aerobic conditions (■————■).

globin concentrations at low ionic strength in the absence of oxygen. These data are not sufficiently accurate to establish that V_{max} is constant but do suggest that V_{max} is relatively stable while the apparent K_D values for the early and late stages of the reduction are vastly different. V_{max} was, therefore, assumed to be constant and taken to be equal to 30 μM/min, K_1 was set at K_D, and the value of K_D that satisfied eq. 7 was determined at various theoretical time points in each reduction.

Plots of K_D vs. the fraction of reduced heme, $\bar{Y}$, are given in fig. 5. At low ionic strength ($I = 0.003$ M) and in the presence of oxygen, a relatively constant value of K_D was obtained throughout the reduction of methemoglobin (fig. 5a). This suggests a constant affinity between cytochrome b_5 and each tetrameric form of hemoglobin. In contrast, analysis of reductions in the absence of oxygen resulted in two values for K_D, a low value early in the reduction and a high value late in the reduction. These two values are approximately an order of magnitude apart and are connected by intermediate values of K_D which define a fairly abrupt transition that occurs at the midpoint of the reduction. In the early part of the reduction the first two terms in eq. 7 predominate and, therefore, the lower value of K_D in this region

characterizes the first two steps of the reduction. Similarly, the high values of K_D characterize the final two steps in the reduction. It follows, then, that the affinity of cytochrome b_5 for H_4 and H_3 is high while the affinity for H_2 and H_1 is low. Each intermediate value of K_D is not a meaningful value but is simply the best single estimate to the fourth-order polynomial representation of eq. 7 when significant amounts of H_3 and H_2 are present simultaneously. When reductions were carried out at higher ionic strength, all values of K_D were increased (fig. 5b) due to the diminished ionic affinity between the two proteins.

Reduction in the presence of oxygen at high ionic strength is more complicated. When hemoglobin is primarily in its ferric form, the K_D value is similar to the low K_D observed in the absence of oxygen. However, the K_D value steadily increases as $\bar{Y}$ increases. This is apparently due to the increasingly significant role of auto-oxidation of cytochrome b_5 as the overall rate of methemoglobin reduction decreases during the course of the reaction. The auto-oxidation is mathematically equivalent to an increased inhibition of the interaction of methemoglobin with cytochrome b_5 and is manifested as an increasing K_D in the calculation.

3.3. Detection of high-spin hydroxymethemoglobin

Using the multiple regression analysis technique (sections 2.4 and 2.7), a previously unrecognized increase in high-spin hydroxymethemoglobin was discovered in partially reduced hemoglobin in the absence of oxygen. The MCD spectrum of this species is shown in fig. 6. The spectrum is distinct from those of aquomethemoglobin and mixed-spin hydroxymethemoglobin at pH 10, but there is a striking similarity to the spectrum of fluoro-methemoglobin. The presence of this species can be seen as a skewing of the 640 nm trough of the high-wavelength charge-transfer band which is normally due to aquomethemoglobin. An enlarged view of the high-wavelength region taken from the midpoint of the reduction in fig. 2a is shown in fig. 7 (dotted line). There is clearly a negative deflection near 620 nm due to the contribution of a signal with a negative maximum at a lower wavelength than that of aquomethemoglobin and close to that of fluoromethemoglobin. Since this species shows charge-transfer bands in similar regions to those of fluoromethemoglobin it is very likely a high-spin form of methemoglobin. In contrast to methemoglobin reduction, metmyoglobin reduction proceeds with a simple monotonic decrease in the 640 nm trough with no skewing in the 610–630 nm region (data not shown).

Analysis of a reduction of methemoglobin at pH 7.8 for mixed-spin hydroxymethemoglobin, aquomethemoglobin, and fluoromethemoglobin (fig. 8) led to tentative identification of the high-
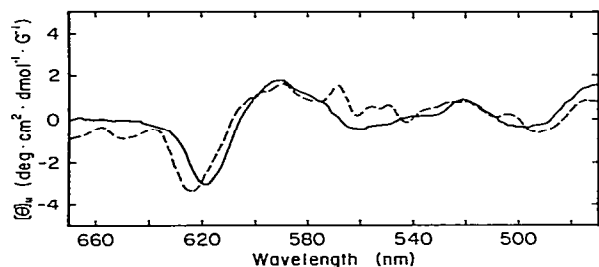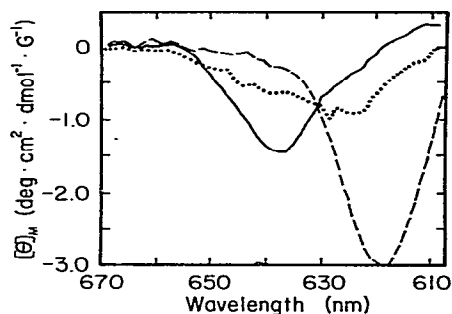

Fig. 7. MCD spectrum of partially reduced methemoglobin showing the contribution of the high-spin species. Methemoglobin was brought to approx. 50% reduction by incubation for 17 min (see fig. 2 and table 1). Low-energy region of the MCD visible spectrum of the partially reduced methemoglobin (· · · · · ·). aquomethemoglobin (———) and fluoromethemoglobin (- - - - - -).

spin component as high-spin hydroxymethemoglobin. As reduction proceeded, the mixed-spin hydroxide signal of methemoglobin decreased and the pure high-spin signal increased in a 1 : 1 relationship, while the fraction of aquomethemoglobin remained constant. Further evidence that the high-spin species is high-spin hydroxymethemoglobin was provided by a study of the effect of pH on levels of high-spin form generated during methemoglobin reduction. A plot of the maximum value for the fraction of methemoglobin present as the high-spin form vs. pH (fig. 9) yielded a set of points that lie along a theoretical titration curve with a pK of 7.78. This is close to the pK_a expected for the aquo-to-hydroxy transition of methemoglobin [18].

During methemoglobin reduction, the absolute amount of high-spin hydroxy derivative is initially zero, increases to a maximum at approximately the midpoint of the reduction, and then declines to zero, paralleling the decrease in total methemoglobin. The fraction of total methemoglobin present as high-spin hydroxide derivative remains constant once the midpoint is reached. The amount of high-spin hydroxide varies with the conditions. At low ionic strength and in the absence of oxygen, the high-spin hydroxide reached a maximum of 10% at 50% reduction (fig. 10a). In the presence of 0.1 M NaCl, a maximum of 12% is reached at 45%

Fig. 6. Calculated MCD spectrum of the high-spin species of mixed-valence hemoglobin. Spectrum calculated as described in section 2.7 (- - - - - -). spectrum of fluoromethemoglobin determined as described in fig. 1 (———).
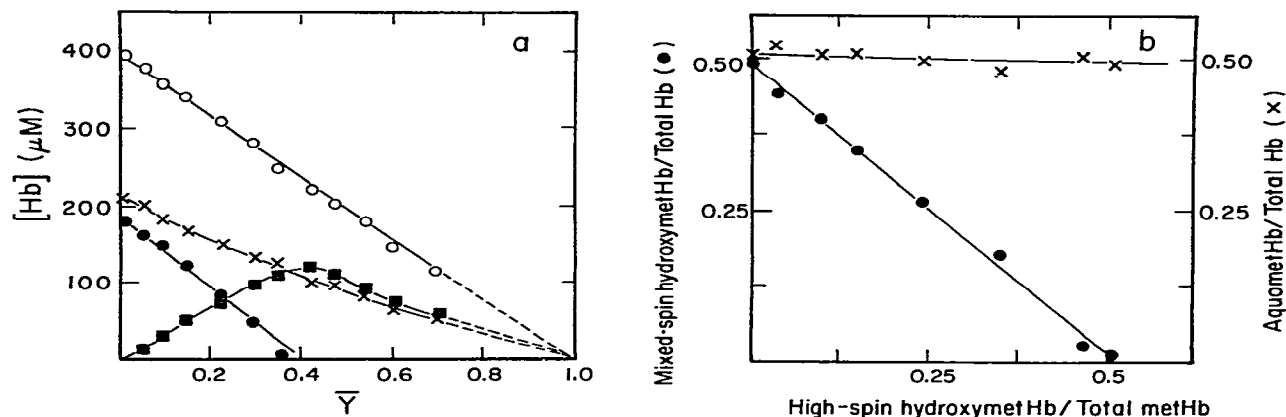
Fig. 8. Changes in the levels of the various species of ferric hemoglobin during the course of methemoglobin reduction. Reduction was carried out in the absence of oxygen at pH 7.8 and 8°C. Final concentrations; 400 μM methemoglobin, 4 μM cytochrome b_5, 0.05 unit cytochrome b_5 reductase/ml, 1 mM NADH, and 10 mM dimethylglutaric acid (pH 7.8). In this multiple regression analysis, methemoglobin at pH 10.0 provided the spectrum of mixed-spin hydroxide methemoglobin, methemoglobin at pH 6.6 provided the spectrum of aquomethemoglobin, and fluoromethemoglobin was used to approximate the spectrum of the high-spin, mixed-valence methemoglobin species. Values for each species were calculated as described in section 2.4. $\overline{Y}$ is the fraction of hemoglobin subunits in the ferrous form. (a) Computed values for concentrations of the various species. Total ferric hemoglobin (O————O), aquomethemoglobin (×————×), mixed-spin hydroxymethemoglobin (●————●), high-spin methemoglobin (■————■). (b) The fraction of total methemoglobin present as the mixed-spin hydroxide species (●————●) and as the aquomethemoglobin species (×———— ×) plotted vs. the fraction of total methemoglobin present as the high-spin species.
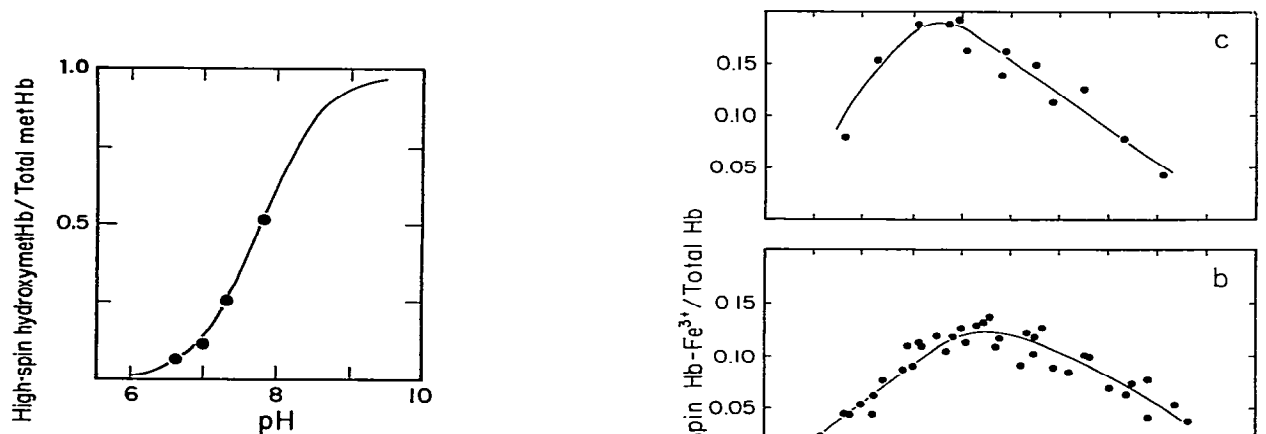

Fig. 9. Effect of pH on the maximum fraction of methemoglobin present as high-spin species during reduction. Conditions and procedures were the same as those described in fig. 8, except for different pH values. The smooth curve is a titration curve for an acid with pK_a = 7.78, calculated from the Henderson-Hasselbalch equation.

Fig. 10. Relationship between high-spin signal and valence state of hemoglobin. Reduction was carried out in the absence of oxygen as described in fig. 3a. $\overline{Y}$ is the fraction of hemoglobin subunits in the ferrous form. (a) No addition; (b) 0.1 M NaCl; (c) 50 μM IHP, with and without NaCl.
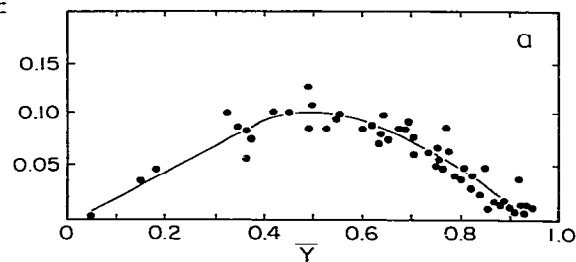
reduction (fig. 10b) and in the presence of IHP at either low or high ionic strength, a maximum of 19% is reached at 35% reduction (fig. 10c). In the presence of oxygen, high-spin hydroxide is detected only in the presence of IHP; under these conditions, a maximum concentration of 12% is seen at 30% reduction (data not shown).

4. Discussion

4.1. MCD spectra of bovine hemeproteins

The observed MCD spectra of the various oxidation and ligand states of bovine hemoglobin are very similar to those reported for human hemoglobin at this pH [5–7]. The spectra of the oxidized and reduced forms of bovine cytochrome b_5 (fig. 1), however, differ in intensity in the visible region from those reported by Dolinger et al. [2] for rat liver cytochrome b_5 and by Vickery et al. [3] for pig liver cytochrome b_5. The Soret region does, however, agree with that obtained by Vickery et al. [1] for calf liver cytochrome b_5, for which the visible region was not reported.

4.2. Reduction kinetics

MCD proved to be an effective way to study the kinetics of methemoglobin reduction. It allowed us simultaneously to follow methemoglobin reduction and to monitor the level of ferrous cytochrome b_5. The intense signal of ferrous cytochrome b_5 allowed such studies to be carried out at low ratios of cytochrome b_5 to hemoglobin concentrations. Multiple regression analysis yielded concentrations of all the species present during the reduction in a reliable and self-consistent manner. The spectrum of each species, taken in the pure, isolated form, adequately represented that species when other forms were present, except in the case of cytochrome b_5.

The α-peak of the spectrum of ferrous cytochrome b_5 showed a narrowing in the presence of forms of hemoglobin. At low ionic strength in the absence of oxygen, the narrowing was approx. 1 nm at the beginning of methemoglobin reduction and 0.5 nm at the completion of the reduction.

Under these conditions, the K_D changes by an order of magnitude (see fig. 5a) which results in about twice as much cytochrome b_5 complexed to hemoglobin at the beginning of the reduction than at the end. This is coincident with the 2-fold change in the narrowing of the cytochrome b_5 signal. The significance of this finding has yet to be explored.

The results of section 3.2 demonstrate that the reduction of methemoglobin tetramer can be interpreted in terms of four apparent first-order rate constants, one for each of the four possible levels of oxidation of tetrameric methemoglobin. These four rate constants were derived in the context of a model that assumed four sequential, nonreversible steps with each step being characterized by a first-order process. The model contains the expectation that the ratio $k_4 : k_3 : k_2 : k_1$ should follow the pattern $4:3:2:1$, which represents the number of available ferric subunits on each of the four possible tetrameric forms [16]. This expectation follows from the hypotheses that the intrinsic reaction rate of ferrous cytochrome b_5 with a ferric hemoglobin subunit is constant for each tetrameric species and that ferrous cytochrome b_5 interacts only with the ferric subunits of hemoglobin. The observed ratio pattern decreased more rapidly than the $4:3:2:1$ pattern in the case of reduction under oxygenated conditions and therefore did not support the hypotheses. Reduction under aerobic conditions is an important test for the hypotheses because there should be no conformational changes in the protein to influence the rate. It is clear that the derived rate constants, while they can generate a curve that fits the data, are not easily interpretable in terms of the assumptions of the model. One is forced to postulate further that nonspecific changes occur as the tetramer passes through each step of the reduction which leads to decreases in the intrinsic ferrous cytochrome b_5-ferric subunit reaction rate. If such changes do occur, this model offers no insight into their origins.

In order to analyze the reduction kinetics from a more realistic approach we formulated the equilibrium state model II. This model postulates the formation of an intermediate, in the form of a protein-protein complex, and the ability of ferrous cytochrome b_5 to form nonproductive complexes

with ferrous hemoglobin subunits. The equilibrium formulation (eq. 7) is based on Michaelis-Menten kinetics incorporating competitive inhibition, an approach used for enzymatic reactions where an enzyme-substrate complex is assumed. Although the electron transfer between cytochrome b_5 and hemoglobin is considered a nonenzymatic step, the separation of this reaction into complexation (k_i') and then electron movement (k_i''') justifies the use of this kinetic approach.

Eq. 7 was able to describe satisfactorily the data for the reductions using the assumptions of a single V_{max} and with K_I equal to K_D. In the presence of oxygen, a constant value of K_D was obtained. This supports the reaction scheme of eq. 8 as well as the assumptions of the model. Although mechanisms cannot be definitively determined by kinetics analysis, this analysis is consistent with the following conclusions: (1) the rate constants of eq. 8 are independent of i; (2) ferrous and ferric hemoglobin subunits have the same affinity for cytochrome b_5; and (3) reaction is a two-step process with the rate of electron movement, k''', being approximately equal to 0.1 s^{-1}. In the absence of oxygen a dramatic increase in K_D for the last two subunits in the reduction was observed. This implies that the ionic interaction between the two proteins is very sensitive to the R-to-T conformational change of hemoglobin. Therefore, the equilibrium competitive model fits the data and yields parameters that are interpretable and consistent with known facts.

The data presented in sections 3.2 and 3.3 make it reasonable to assume that the structural transition, which occurs when two subunits of the tetramer are reduced, alters the structure of the two ferric subunits both externally and at the heme centers. The external changes in conformation result in lowered affinity for cytochrome b_5, as represented by the increased K_D. The change at the heme results in the complete conversion of the hydroxide methemoglobin component to a high-spin form. Whereas the external change affects the rate of reduction, the change of spin state does not seem to alter the electron-transfer step in the reduction, since V_{max} is the same before and after this structural transition (fig. 4). Therefore, the ionic interaction between the two proteins is sensi-

tive to tertiary structure and is the primary modulator of the reduction rate.

Results of reductions performed in the presence of IHP were difficult to interpret. In the presence of IHP and at 0.1 M ionic strength under anaerobic conditions, the transition point from low to high K_D occurred prior to 50% reduction, but neither model I nor II was capable of satisfactorily fitting the data. In agreement with published data [19], the α- and β-subunits appear to show a marked difference in affinity for cytochrome b_5 in the presence of IHP, with the result that eight rate constants in model I or eight terms in eq. 7 for model II are needed to describe the reduction.

4.3. High-spin hydroxymethemoglobin

The high-spin methemoglobin that occurred in increased amount during reduction appeared to be a form of hydroxymethemoglobin. Hydroxymethemoglobin exists as a thermodynamic mixture of high- and low-spin states [20] both of which are represented in the MCD spectrum of hydroxymethemoglobin at pH 10.0 (fig. 1). The band at 575 nm is a characteristic low-spin band, while the negative deflection at 620 nm is part of a band centered near 600 nm representing the high-spin component. During the reduction of bovine methemoglobin the intensity of the low-spin band decreases and that of the high-spin band increases. When we analyzed the data, using hydroxymethemoglobin at pH 10 to represent the mixed-spin species and fluoromethemoglobin to represent the pure high-spin hydroxymethemoglobin, the mixed-spin species was found to be replaced by the high-spin species in a 1:1 relationship during the reduction. This demonstrates that the spectra of fluoromethemoglobin, the high-spin component of mixed-spin hydroxymethemoglobin, and the high-spin species generated during the reduction, are all very similar and supports our hypothesis that the generated species is high-spin hydroxymethemoglobin. This hypothesis is further supported by the increase in absolute level of this species at high pH.

The occurrence of the maximum concentration of the high-spin component near the midpoint of the reduction suggests that this component was the

result of ferric subunits being driven to a higher spin state by structural changes induced by the ferrous subunits. The percent of ferric hemoglobin present as the high-spin hydroxide species reached a stable maximum beginning near the midpoint of the reduction (table 1). This indicates that a constant conformational 'pressure' was present during the second half of the reduction and is consistent with the transformation of the tetramer to the T-state. The effect of the allosteric effector, IHP, to increase the amount of high-spin hydroxide at earlier points in the reduction (fig. 3c) supports the above hypothesis since IHP can induce a T-like state in methemoglobin. The data support the model of Perutz et al. [21] that links spin state to structural conformation.

The existence of the high-spin hydroxide form as a component of methemoglobin has been discussed by Antonini and Brunori [14] and the expected absorption spectrum of pure high-spin hydroxymethemoglobin has been calculated by George et al. [22]. Near neutral pH, however, the predominant methemoglobin form is the high-spin aquo species with smaller contributions of low-spin aquo, low-spin hydroxide, and high-spin hydroxide forms. In partially reduced hemoglobin, Perutz [23] detected an increase in methemoglobin spin state and attributed it to an increase in the high-spin hydroxide form. Moreover, Perutz et al. [18] have shown that T-state methemoglobin, induced by IHP, exhibited a hydroxide component of higher spin. The spectrum of this species was not obtained, however, because IHP does not bind at high pH where the hydroxide component predominates and methemoglobin thus remains in the R-state. In the current study, we establish an approximate MCD spectrum of this species (fig. 6) which resembles the spectrum of fluoromethemoglobin. The differences in the two spectra, which occur at the prominent charge-transfer bands at 620 and 500 nm [24,25], may have arisen from the analytical procedures used to determine this spectrum. In fact, a closer similarity to the fluoromethemoglobin spectrum may be inferred from the excellent fit to the data (table 1 and fig. 8) generated by the use of fluoromethemoglobin as the putative high-spin hydroxide form. A similar agreement was calculated by George et al. [22] for

the absorption band components of fluoro- and high-spin hydroxymethemoglobin. The MCD spectrum of high-spin hydroxymethemoglobin, being similar to that for the fluoride methemoglobin, thus verifies this calculated spectrum and indicates that the high-spin hydroxide species, like the fluoride derivative, exists completely in a spin state of 5/2.

The detection of the high-spin hydroxide species was made possible because the mixed-valence state that is generated during anaerobic reduction induces a T-state conformation in bovine hemoglobin that results in the conversion of the hydroxymethemoglobin component to the completely high-spin state. The tetramer-dimer association constant for bovine hemoglobin $(4 \times 10^6$ $M^{-1})$ [15], which is an order of magnitude greater than that for human hemoglobin, may be responsible for this. In limited experiments we detected a smaller increase in high-spin hydroxymethemoglobin during the reduction of human methemoglobin. The subunit interactions that give rise to the different association constants are possibly responsible for the observed difference in the amount of high-spin hydroxymethemoglobin, making bovine hemoglobin an interesting protein for future work.

Acknowledgements

References

1 L. Vickery, T. Nozawa and K. Sauer, J. Am. Chem. Soc. 98 (1976) 351.
2 P.M. Dolinger, M. Kielczewski, J.R. Trudell, G. Barth, R.E.

Linder, E. Bunnenberg and C. Djerassi, Proc. Natl. Acad. Sci. U.S.A. 71 (1974) 399.

3 L. Vickery, A. Salmon and K. Sauer, Biochim. Biophys. Acta 386 (1975) 87.

4 M. Kajiyoshi and F.K. Anan, J. Biochem. 81 (1977) 1327.

5 Y.A. Sharonov, A.P. Mineyev, M.A. Livshitz, N.A. Sharonova, V.B. Zhurkin and Y.P. Lysov, Biophys. Struct. Mech. 4 (1978) 139.

6 J.I. Treu and J.J. Hopfield, J. Chem. Phys. 63 (1975) 613.

7 R.E. Linder, R. Records, G. Bart, E. Bunnenberg, C. Djerassi, B.E. Hedlund, A. Rosenberg, L. Seamans and A. Moscowitz, Biophys. Chem. 12 (1980) 143.

8 P.G. Righetti, G. Gacon, E. Gianazza, D. Lostanlen and J.-C. Kaplan, Biochem. Biophys. Res. Commun. 85 (1978) 1575.

9 D.E. Hultquist, L.J. Sannes and D.A. Schafer, Prog. Clin. Biol. Res. 55 (1981) 291.

10 M.R. Mauk and A.G. Mauk, Biochemistry 21 (1982) 4730.

11 D.A. Schafer and D.E. Hultquist, Biochem. Biophys. Res. Commun. 95 (1980) 381.

12 L. Spatz and P. Strittmatter, J. Biol. Chem. 248 (1973) 793.

13 J. Ozols, Biochemistry 13 (1974) 426.

14 E. Antonini and M. Brunori, Hemoglobin and myoglobin in their reactions with ligands, Frontiers of biology, vol. 21 (North-Holland, Amsterdam, 1971) p. 3.

15 S. Hanlon, G. Nagel, R. Boyd, R. Lewshenia, M. Forsberg and S. Cheung, Biochim. Biophys. Acta 229 (1971) 359.

16 P.R. Bevington, Data reduction and error analysis for the physical sciences (McGraw-Hill, New York, 1969).

17 J.S. Olson, Methods Enzymol. 76 (1981) 652.

18 M.F. Perutz, J.K.M. Sanders, D.H. Chenery, R.W. Noble, R.R. Pennelly, L.W.M. Fung, C. Ho, I. Giannini, D. Pörschke and H. Winkler, Biochemistry 17 (1978) 3640.

19 A. Tomodo, T. Yubisui, A. Tsuji and Y. Yoneyama, J. Biol. Chem. 254 (1979) 3119.

20 M. Kotani, Adv. Quant. Chem. 4 (1968) 227.

21 M.F. Perutz, E.J. Heidner, J.E. Ladner, J.G. Beetlestone, C. Ho and E.F. Slade, Biochemistry 13 (1974) 2187.

22 P. George, J. Beetlestone and J.S. Griffith, in: Haematin enzymes (part I), eds. J.E. Falk, R. Lemberg and R.K. Morton (Pergamon Press, Oxford, 1961) p. 105.

23 M.F. Perutz, Nature 237 (1972) 495.

24 D.W. Smith and R.J.P. Williams, Struct. Bond. 7 (1970) 1.

25 T. Nozawa, S. Ookubo and M. Hatano, J. Inorg. Biochem. 12 (1980) 253.